Magnetic Core Shape Design by the Sampled Pattern Matching Method

Hideo Saotome*, Jean-Louis Coulomb**, Yoshifuru Saito*** and Jean-Claude Sabonnadiere**

* Dept. of Elect. & Electron. Engng., Chiba University, Inage, Chiba 263, JAPAN
** L.E.G. (INPG CNRS URA 355), ENSIEG, BP46, 38402 St Martin d'Heres Cedex, FRANCE
*** College of Engineering, Hosei University, Kajino, Koganei, Tokyo 184, JAPAN

Abstract **— This paper presents a novel objective function in order to design electromagnetic devices. The finite element method taking the open boundary condition into account is used for magnetic field computation. Comparison of the results obtained with the novel objective function and the least squares shows that the former is superior to the latter.**

I. Introduction

Designing an electromagnetic device from its specification is reduced to solving the inverse problem. This work has been done by experienced designers. It is very much expected that designing will be automatically carried out by computers in the near future. In order to realize it, various studies have proposed designing methodologies [1-4]. In the previous studies, the least square evaluation has been widely used as the objective function. This method corresponds to minimizing the distance between target and evaluation vectors in the linear space.

For the purpose of analyzing the inverse problem, the sampled pattern matching (SPM) method in which we minimize the angle of the two vectors has been developed [5-8]. In this paper, we apply the SPM method using the finite element method (FEM) on the open magnetic field condition to electromagnetic device designing. A simple example of magnetic core shape design is demonstrated.

II. A Novel Objective Function

Electromagnetic fields can be expressed by

$$\mathbf{A}\,\mathbf{x} = \mathbf{b}, \tag{1}$$

where the vectors $\mathbf{x}$ and $\mathbf{b}$ denote the field (or potential) and its source distributions, respectively. The system matrix $\mathbf{A}$ which is determined by geometry and medium parameters has some unknowns in electromagnetic device design problems where the vector $\mathbf{x}$ is known as a target value $\mathbf{x}_t$. Numerous studies have devoted their efforts to determining $\mathbf{A}$ by means of the least squares, i.e. minimizing the error

$$\varepsilon_r = \| \mathbf{x}_t - \mathbf{x}_e \| / \| \mathbf{x}_t \|, \tag{2}$$

where the field vector $\mathbf{x}_e$ being evaluated is given by (1) with trial design parameters.

In this paper, a novel objective function

$$\gamma = \mathbf{x}_t^T \cdot \mathbf{x}_e \,/\, (\| \mathbf{x}_t \| \, \| \mathbf{x}_e \|), \tag{3}$$

which we maximize is proposed for magnetic core shape design. The magnetic field evaluation based on (3) has been applied to inverse problems in biomagnetic fields [5-7] and the non-destructive testing [8].

The most notable difference between (2) and (3) is as follows. The former depends on the norm of $\mathbf{x}_e$, i.e. the norm of $\mathbf{b}$ in (1), whereas the latter does not, because γ of (3) gives a normalized vector element pattern matching rate between $\mathbf{x}_t$ and $\mathbf{x}_e$. When $\mathbf{x}_e/\|\mathbf{x}_e\|$ coincides with $\mathbf{x}_t/\|\mathbf{x}_t\|$, γ becomes 1. Even if we assume the field source vector $k\mathbf{b}$ where k is an arbitrary scalar, the normalized field vector $\mathbf{x}_e/\|\mathbf{x}_e\|$ obtained by (1) is independent of k. However, ε_r of (2) depends not only on $\mathbf{x}_e/\|\mathbf{x}_e\|$ but also on k.

Let us consider the error defined by

$$E_r = \| (\mathbf{x}_t/\|\mathbf{x}_t\|) - (\mathbf{x}_e/\|\mathbf{x}_e\|) \|. \tag{4}$$

When we assume $\mathbf{x}_t$ and $\mathbf{x}_e$ are n dimensional column vectors:

$$\mathbf{x}_t = [x_{t1} \quad x_{t2} \quad \cdots \quad x_{tn}]^T, \tag{5}$$

$$\mathbf{x}_e = [x_{e1} \quad x_{e2} \quad \cdots \quad x_{en}]^T, \tag{6}$$

we have

$$E_r^2 = \sum_{i=1}^{n} \{(x_{ti}/\|\mathbf{x}_t\|) - (x_{ei}/\|\mathbf{x}_e\|)\}^2 = 2 - 2\gamma. \tag{7}$$

Therefore, maximizing γ of (3) is exactly equal to minimizing the error E_r of (4). However, it is different from minimizing the conventionally used error ε_r of (2).

0018-9464/95$04.00 © 1995 IEEE

III. FEM on the Open Boundary Condition

In order to analyze the magnetic field on the open boundary condition, one of the authors developed the strategic dual image (SDI) method using the FEM [9,10]. The SDI method has been generalized as field source transformations between the inside and the outside of a finite region [11,12]. In two dimensional open magnetic field problems, the SDI method sets a circular boundary line containing all the field sources. This method needs only one condition that summation of positive and negative values of all the field sources inside the circular line must be zero. Imposing the zero and natural boundary conditions on the circular boundary and averaging the obtained vector potentials at the same node give solutions on the open field condition.

In the next chapter, we will use the finite element mesh shown in Fig. 1 for two dimensional magnetic core shape design which is one of the open field problems. In order to verify the accuracy of solutions obtained with the mesh of Fig. 1, having 580 triangles and 321 nodes, we compare the functional values obtained with it and a finer mesh having 1940 triangles and 1015 nodes inside the same boundary. In the homogeneous open field, the functional value obtained with the mesh of Fig. 1 is 99.2% with respect to the one obtained with the finer mesh when uniform current density is given in the region (x=52~68, y=0~64), which concludes that the mesh of Fig. 1 is valid for the design.

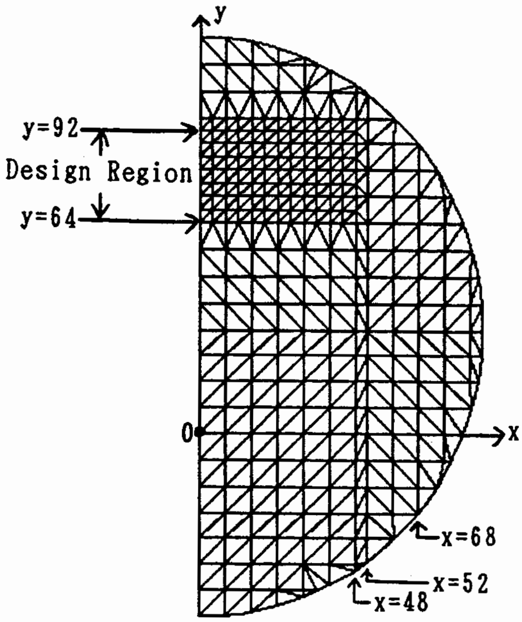

Fig. 1. Finite element mesh of the SDI method.

IV. An Example and Its Design Process

An example specification for magnetic core shape design is uniform magnetic flux density B_y and $B_x=0$ on the target surface in the two dimensional magnetic field shown in Fig. 2. The configuration of the DC exciting coils and the magnetic material is symmetrical with respect to the y-axis, but exciting current flowing directions in the positive and negative x regions are opposite each other. Let us assume that the magnetic material has the constant relative permeability $\mu_r=500$.

In optimization problems, a trajectory of reaching a goal takes an important role, so that various methodologies of determining it have been proposed [1-4]. However, in this paper, we applied a very simple algorithm to the design in order to clarify the difference between the SPM and least square methods. The rectangular design region of Fig. 2 is divided into 168(=14x12) small triangular elements as shown in Fig. 1. We accumulate triangle elements of $\mu_r=500$ on the top surface of the initial shape of the magnetic material. The magnetic flux densities B_x and B_y on the target surface (x=0~32, y=94) are obtained from the potential gradients in their triangular elements. As a result, the conventional least square (CLS) error ε_r and the SPM rate γ are calculated by (2) and (3), respectively. By selecting the best element giving the maximum γ from the first layer, we have a new contour surface including it. Then, we accumulate the next best element on the contour. Similarly, continuing the best selection of the elements which give the minimum ε_r is

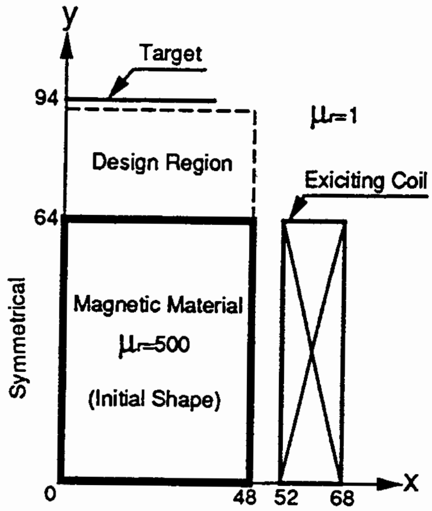

Fig. 2. Configuration of an example.

carried out in the CLS method. These processes are stopped at the first peaks of the γ maximum and the ε_r minimum, respectively.

Fig. 3 shows comparison of the target fields designed by the SPM and CLS methods. In the SPM method, it is not necessary to decide the amplitude of the exciting current before computation, because γ of (3) is independent of $\|\mathbf{x}_e\|$. However, the amplitude must be presupposed in the CLS method. In this paper, we assumed two amplitude values of the exciting current for the CLS method. In the first case (CLS*), the amplitude is adjusted and fixed to having B_{ymax}=100% in the initial shape. In the second case (CLS#), it keeps the same value as the SPM result (121% of the first case) obtained with the ratio $\|\mathbf{x}_t\|/\|\mathbf{x}_e\|$ at the final step in the SPM design process. The field errors, defined by (2), in the initial and designed shapes (Fig. 4) are listed in Table 1. The SPM method provided the best result among them.

From the results shown in Fig. 3, it is observed that the uniformity of B_y is sacrificed for reducing B_x in all the cases. However, the SPM method gave the smallest average displacement of B_x from its target B_x=0%. This result is explained as follows. Let us consider the error e_r defined by

$$e_r^2 = \sum_{i=1}^{n} \{w_i (x_{ti} - x_{ei})^2\}, \quad (8)$$

where $w_i\,(i=1,2,\cdots,n)$ are weight coefficients depending on i. If we obtain w_i for $i=1,2,\cdots,n$ by assuming e_r of (8) equals E_r of (7), i.e.

$$w_i (x_{ti} - x_{ei})^2 = \{(x_{ti}/\|\mathbf{x}_t\|) - (x_{ei}/\|\mathbf{x}_e\|)\}^2, \quad (9)$$

the coefficients for B_x are much larger than

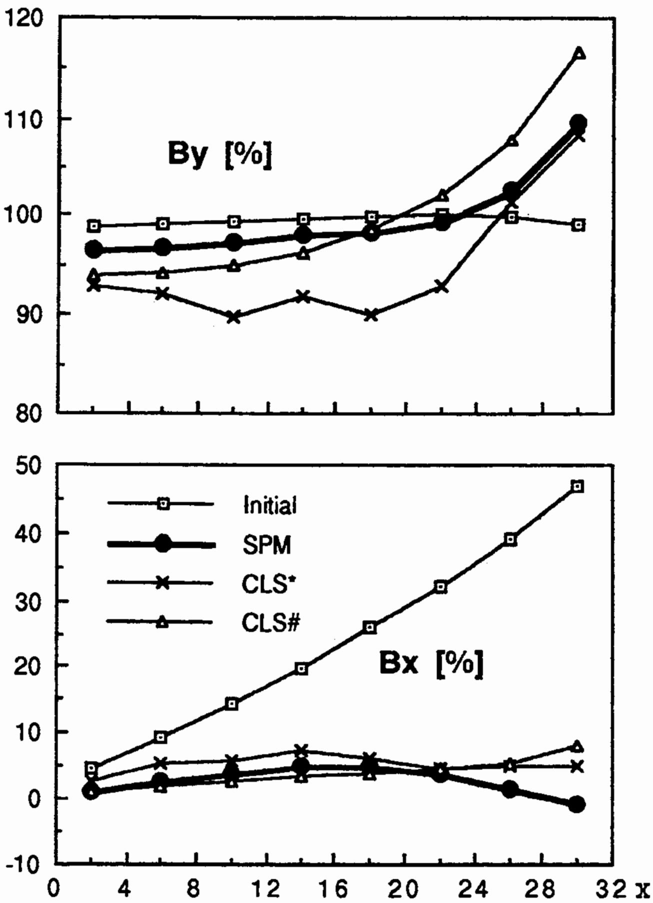

Fig. 3. Comparison of the target fields designed by different objective functions.

Table 1. RMS errors of the designed fields.

Core shape	Initial	SPM	CLS*	CLS#
RMS error [%]	27.8	5.5	9.5	8.8

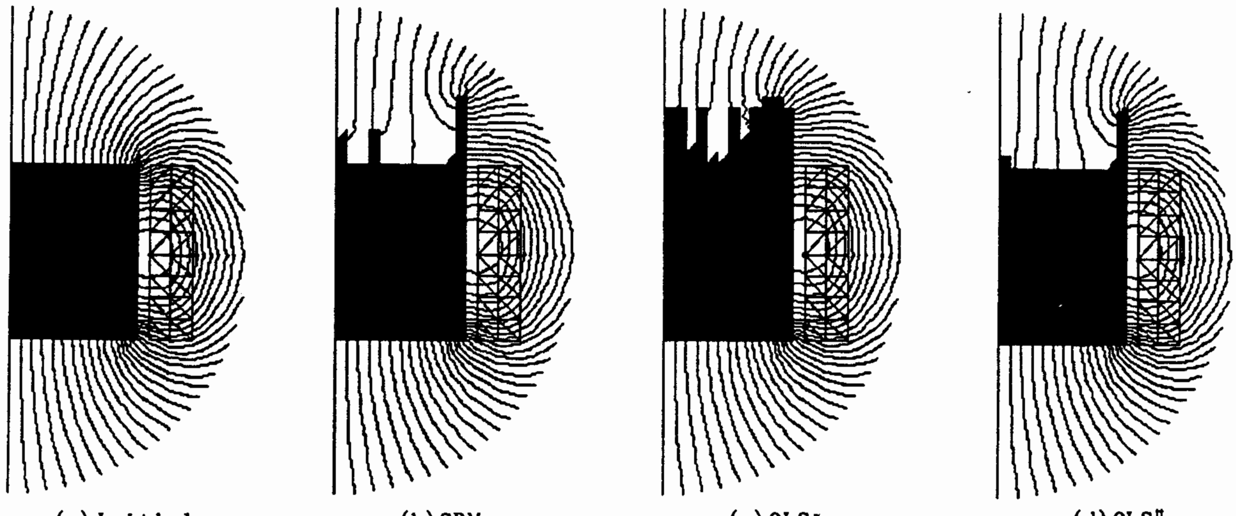

(a) Initial (b) SPM (c) CLS* (d) CLS#

Fig. 4. Initial and designed core shapes and the vector potentials.

those for B_y (see Appendix) whereas they are constant in the case of (2). As a result, the SPM method laid stress on reducing B_x. On the other hand, the SPM method gave the smallest displacement of B_y from B_y=100%, because the amplitude of the exciting current has been suitably determined by the norm ratio $\|\mathbf{x}_t\| / \|\mathbf{x}_e\|$.

V. Conclusion

The design process using the CLS method simultaneously requires both medium and source parameters in the field. This means, in the CLS method, field source amplitude considerably affects the design process and its result.

In the SPM method, medium geometry and field source amplitude are independently evaluated. In other words, the SPM method automatically assumes the best amplitude value of the field source for each geometry in the design process. This feature enables us to have a simple algorithm which needs less CPU time in the design of electromagnetic devices.

Appendix

As an example of determining w_i in (8), let us assume that the two dimensional field vector $\mathbf{x}=[B_x \ B_y]^T$:

$$\mathbf{x}_t = [0 \quad 100]^T, \tag{10}$$
$$\mathbf{x}_e = [1 \quad 101]^T, \tag{11}$$

where the differences of element values for i=1 and 2 are the same value 1. The coefficients $w_1=9.80\times10^{-5}$ and $w_2=2.40\times10^{-9}$ are respectively obtained by (9). In this case, w_1 for B_x is considerably larger than w_2 for B_y.

References

[1] M.Enokizono, T.Todaka and H.Etoh, "Three-dimensional boundary element method with shape modification," *Int. J. Appl. Electromag. Matrls.*, Elsevier, vol.2, pp.73-79, 1991.

[2] C.S.Koh, S.Y.Hahn, K.S.Lee and K.Choi, "Design sensitivity analysis for shape optimization of 3-d electromagnetic devices," *IEEE Trans. Magn.*, vol.MAG-29, no.2, pp.1753-1757, March 1993.

[3] K.Weeber and S.R.H.Hoole, "The subregion method in magnetic field analysis and design optimization," *IEEE Trans. Magn.*, vol.MAG-28, no.2, pp.1561-1564, March 1992.

[4] A.Gottvald, "Comparative analysis of optimization methods for magnetostatics," *IEEE Trans. Magn.*, vol.MAG-24, no.1, pp.411-414, January 1988.

[5] Y.Saito, E.Itagaki and S.Hayano, "A formulaion of the inverse problems in magnetostatic fields and its application to a source position searching of the human eye fields," *J. Appl. Phys.* vol.67, no.9, pp.5830-5832, May 1990.

[6] H.Saotome, K.Kitsuta, S.Hayano and Y.Saito, "A neural behavior estimation by the generalized correlative analysis," *IEEE Trans. Magn.*, vol.MAG-29, no.2, pp.1389-1394, March 1993.

[7] H.Saotome, K.Kitsuta, S.Hayano and Y.Saito, "Electromagnetic field source searching from the local field measurement," *Int. J. Appl. Electromag. Matrls.*, Elsevier, vol.3, no.4, pp.297-306, April 1993.

[8] H.Saotome, T.Doi, S.Hayano and Y.Saito, "Crack identification in metallic materials," *IEEE Trans. Magn.*, vol.MAG-29, no.2, pp.1861-1864, March 1993.

[9] Y.Saito, K.Takahashi, and S.Hayano, "Finite element solution of open boundary magnetic field problems," *IEEE Trans. Magn.*, vol.MAG-23, no.5, pp.3569-3571, September 1987.

[10] Y.Saito, K.Takahashi, and S.Hayano, "The strategic dual image method: An extremely simple procedure for open field problems," *J. Appl. Phys.* vol.63, no.8, pp.3366-3368, April 1988.

[11] D.A.Lowther, E.Freeman and B.Forghani, "A sparse matrix open boundary method for finite element analysis," *IEEE Trans. Magn.*, vol.MAG-25, no.4, pp.2810-2812, July 1989.

[12] X.Brunotte, G.Meunier and J.F.Imhoff, "Modelisation elements finis de l'infini par transformation: une alternative rigoureuse, puissante et simple aux methodes hybrides," J.SEE, *Modelisation numerique 3D dans les systemes electromagnetiques*, Gif sur Yvette, ESE, Mars 1991.